Bull. Mater. Sci., Vol. 38, No. 3, June 2015, pp. 617–623. © Indian Academy of Sciences.

Synthesis and characterization of ZnO/TiO_2 composite core/shell nanorod arrays by sol–gel method for organic solar cell applications

K AHMADI[1,2], ALI ABDOLAHZADEH ZIABARI[2,*], K MIRABBASZADEH[1] and A AHADPOUR SHAL[3]

[1]Department of Physics, Amirkabir University of Technology, P.O. Box 15875-4413, Tehran, Iran
[2]Nano Research Lab, Lahijan Branch, Islamic Azad University, P.O. Box 1616, Lahijan, Iran
[3]Department of Electronic Engineering, Faculty of Engineering, Lahijan Branch, Islamic Azad University, P.O. Box 1616, Lahijan, Iran

MS received 22 May 2014

Abstract. **ZnO/TiO_2 core/shell nanorod arrays were deposited on indium tin oxide (ITO) substrate via a facile sol–gel dip-coating process. Effects of solution pH for ZnO, annealing temperature, growth time and temperature on the physical properties of nanorods have been investigated. X-ray diffraction (XRD) analysis and scanning electron microscopy (SEM) were employed to characterize the structural and morphological properties of the prepared composite nanorods. XRD result revealed wurtzite structure of ZnO with a mixed anatase and rutile structure phase for TiO_2. Energy-dispersive X-ray (EDX) and UV–vis spectroscopy were used to study the chemical composition and optical properties of the films, respectively. Electrical resistivity of the films was also investigated. The optical and electrical properties of the bare TiO_2 thin film and core/shell composite were compared together. The results showed that owing to smaller band gap and lower resistivity, the core/shell structure as an electron transport layer for inverted photovoltaic devices is more suitable than bare TiO_2 thin film.**

Keywords. **Organic solar cells; ZnO/TiO_2 core/shell; nanorod arrays; sol–gel.**

1. Introduction

Organic solar cells have attracted considerable attention owing to their potential for large-scale production, flexibility, lightweight and low consumption materials by solution processing.[1] The inverted device architecture in organic solar cell configurations has higher lifetime than the conventional architecture because of the usage of air-stable high-work-function metal as the anodic electrode for hole collection.[2] In this structure, a cathode (e.g., indium tin oxide (ITO)) is used to collect electrons and a metal oxide is used as the electron selective contact at the ITO interface.[3] Owing to high optical transmission in Vis–NIR region and also high carrier mobility, n-type metal oxides such as ZnO and TiO_2 are used in ITO interface.[4] As a clean photoelectric conversion, renewable and potential alternative to the traditional photovoltaic devices, dye-sensitized solar cells (DSSCs) based on nanocrystalline porous TiO_2 thin films for enhanced efficiency were investigated in the recent years. Despite large surface area for dye adsorption, TiO_2 nanoparticle film shows relatively slow electron transport rate, resulting from multiple trapping/detrapping events occurring within grain boundaries that can lead to the high interface recombination reactions and limit the device efficiency.

Effective exciton dissociation and fluent carrier transport into the collecting electrode have a considerable influence on the conversion efficiency of the inverted organic solar cells. Therefore, it is essential to have information on the appropriate energy level of the collecting electrode to match the active layer as the top-contact hole collecting layer. Conduction band energy of ITO has a large barrier height with lowest unoccupied molecular orbital (LUMO) of the active layer. As such, it is unsuitable for electron collecting layer. For this reason, some authors have suggested the extra electron collecting layers like titanium oxide (TiO_2) or zinc oxide (ZnO) due to their suitable (LUMO) positions.[5,6] Oxide semiconductor nanostructures can be used in photonic devices, sensors, solar cells, etc.[7–9] Among these remarkable materials, ZnO and TiO_2 are the most versatile ones because of their non-toxicity, stability and ease to prepare.[10]

Nanostructured materials possess a large surface to volume ratio compared to that of bulk materials.[11–13] They can be prepared as one-dimensional nanostructures like nanorods, nanowires and nanotubes to enhance the surface area. Moreover, these materials can potentially supply a straight transport pathway for charge carriers in photovoltaic cells.[14] The review of literature reveals a rising interest in the new designs of nanoporous electrode based on the core/shell configuration.[15–17]

It is well known that the electron transport rate in ZnO nanorods is much faster than TiO_2 due to its higher electrical

*Author for correspondence (ali_abdolahzadeh@liau.ac.ir)

conductivity.[18] DSSCs based on one-dimensional ZnO nanostructures, which present significantly higher electron mobility than that of both TiO_2 and ZnO nanoparticle films,[19] have in recent times been attracting increasing attention.[20,21] In the present study, we have grown one-dimensional ZnO nanorods by the facile sol–gel route and used the prepared ZnO nanorods as the core to prepare arrays of ZnO/TiO_2 core/shell nanorods (ZTNA) on ITO-coated substrate. The effects of annealing temperature, growth time, growth temperature and solution pH for ZnO on the optical and electrical properties of the prepared nanorods have been investigated fundamentally and the physics related to the possible correlations have been discussed with given reasons.

2. Experimental

All chemicals were purchased from Merck. To prepare ZnO nanorod arrays, thin ZnO seed layers were initially prepared onto ITO substrates by dip-coating process and the coated substrates were suspended vertically in an open beaker of ZnO aqueous solution to grow the rods. Ammonia hydroxide solution was used to adjust the pH value. To prepare TiO_2 shell layers, the obtained ZnO nanorod arrays were dip coated with TiO_2 sol at room temperature. Schematic representation of the mentioned experimental process is given in figure 1.

2.1 *Synthesis of ZnO seed layers*

To prepare ZnO seed layer, 0.5 g of $Zn(Ac)_2{\cdot}2H_2O$ was dissolved in a mixture of 100 ml ethylene glycol ($C_2H_6O_2$) and 5 ml deionized water and stirred for 30 min at 140°C while a stable and homogeneous solution was obtained. ITO-coated glass was used as the substrate and cleaned by sonication in acetone, ethanol and deionized water, prior to use. The cleaned glass substrate immersed into ZnO solution at the rate of 3 cm min^{-1}. Subsequently, the substrate was dried in air and annealed at 150°C for 1 h in a muffle furnace. This process was repeated three times to produce ZnO seed layer.

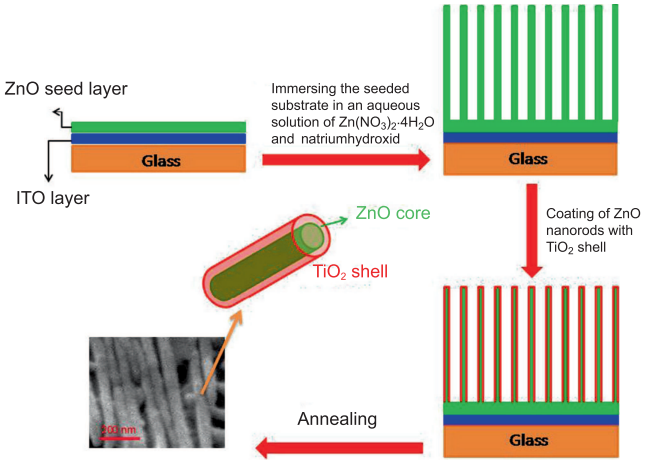

Figure 1. Fabrication of ZnO/TiO_2 core/shell nanorod films by the sol–gel dip-coating method.

2.2 *Growth of well-aligned ZnO nanorod arrays*

Vertical nanorod arrays were grown by immersing the seeded substrates in an aqueous solution of 0.05 g zinc nitrate tetrahydrate and 0.8 g natriumhydroxid dissolved in 200 ml of deionized water. This procedure lasted about 1 h at 70°C and finally the substrate was dried in air.

2.3 *Coating of ZnO nanorods with TiO_2 shell*

Firstly, TiO_2 sol comprising of 8.7 ml tetrabutylorthotitanate and 2.8 ml ethanolamine dissolved in 35 ml ethanol was stirred for 2 h at room temperature. During the stirring, a mixture of 0.45 ml deionized water and 4.5 ml ethanol was added dropwise to the above solution. The prepared sol was aged under light exclusion for 24 h. Thereafter, ZnO-coated layers were immersed in the above prepared sol for 1 min before dip-coating process being started. Subsequently, the substrates were dip coated into TiO_2 sol at the rate of 3 cm min^{-1}. The as-deposited films then were dried in a muffle furnace in air and annealed at 450°C for 1 h and eventually left to be cooled down to room temperature.

3. Characterization

The structure of the prepared films was studied by the X-ray diffraction (XRD) method using a XRD6000, Shimadzu system with CuKα radiation (0.15406 nm). Quantitative analyses were obtained by an energy-dispersive X-ray (EDX) analysis (LEO, 1430VP) with accelerating voltage 17 kV. Surface morphology of the films was studied by scanning electron microscopy (SEM) with a HITACHI S4160 instrument. The spectral optical transmittance T was measured at normal incidence in UV–Vis–NIR spectral region (200–800 nm) with Varian Cary 100 spectrophotometer. The film thickness was measured by a contact profilometer (Dektak 8000). The d.c. electrical resistivity of the samples were measured by Keithley, USA, K361 and IV-CV-Parameter Analyzer.

4. Results and discussion

To do a comprehensive study on the electrical and optical properties of the material, different conditions were tested (table 1). The variations of pH value, growth time, growth temperature and annealing temperature have been studied and shown in detail in table 2.

4.1 *Structural and morphological studies*

Figure 2 shows the representative XRD pattern of ZnO/TiO_2 core/shell nanorod (sample number 3) deposited on ITO-coated glass substrate. The peak at $2\theta = 34.56°$ corresponds

Table 1. Sample number and corresponding experimental parameters that have been changed in the study.

Sample	pH value	Growth time (h)	Growth temperature (°C)	Annealing temperature (°C)
1–5	Variable	1	70	150
6–9	9.5	Variable	70	150
10–13	9.5	1	Variable	150
14–17	9.5	1	70	Variable

Table 2. Values of pH, growth time (G), growth temperature (T_G), annealing temperature (T_A) and thickness (d) for the prepared ZnO/TiO$_2$ core/shell nanorod arrays on ITO substrate.

Sample	pH	d (nm)	Sample	G (h)	d (nm)	Sample	T_G (°C)	d (nm)	Sample	T_A (°C)	d (nm)
1	6.45	380	6	0.5	250	10	45	406	14	150	496
2	8.50	238	7	1	240	11	55	425	15	250	413
3	9.50	336	8	1.5	386	12	65	470	16	350	263
4	10.30	353	9	2	547	13	75	490	17	450	190
5	11.30	234									

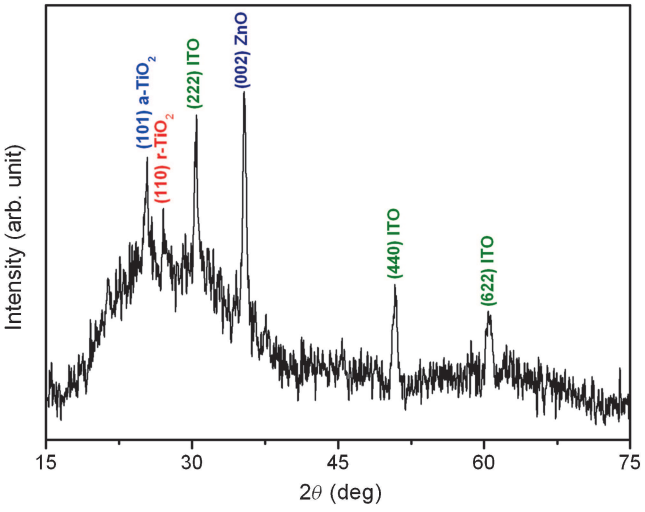

Figure 2. Typical XRD pattern for ZnO/TiO$_2$ core/shell nanorod film (sample number 3 as described in the text).

to diffraction from (002) plane of ZnO hexagonal wurtzite structure which is in good agreement with JCPDS card no. 79-0208. Moreover, it is just the only main peak for ZnO as the core-shell, indicating the presence of preferred orientation and no phase related to other oxides. After deposition of TiO$_2$ as the shell material, an anatase phase with preferred (101) orientation at $2\theta = 25.42°$ was observed (JCPDS card no. 89-4921). Other less intense diffraction peak corresponding to (110) is assigned well to rutile (JCPDS card no. 89-4202) crystalline phase of TiO$_2$. These results revealed that the shell formation on ZnO nanoparticles is a TiO$_2$ layer with a mixed anatase and rutile structure. Peaks from ITO-coated glass substrate are also observed at (222), (440) and (622) planes.

The preparation of initial ZnO nanorods as the core and successful formation of TiO$_2$ as the shell on ITO were observed by SEM. Figure 3a and b presents SEM images of the seed layer and ZnO nanorod arrays, respectively. From figure 3a the average size of the seed grains is around 40 nm. Figure 3b shows the formation of core ZnO nanorods. SEM images of ZnO/TiO$_2$ composite core/shell nanorods are shown in figure 3c. These images clearly show the formation of nanorod arrays. From the figure, the core/shell nanorods have a circular cross-section with an average diameter of about 50 nm.

The chemical composition of the nanorods was determined using EDX spectroscopy and the representative spectrum for sample number 3 is shown in figure 4. The result exhibits the presence of Zn, Ti and In picks with Zn/Ti/In atomic percentage of 14.96/29.35/4.89. These ratios are very close to the nominal values that were calculated to prepare the starting solutions.

4.2 *Electrical and optical properties*

Figure 5 shows the photocurrent voltage characteristics of the cells based on bare ZnO and TiO$_2$-coated ZnO systems. In terms of the device power conversion efficiency, there are different resistances in the system, such as the electrolyte/TiO$_2$ interface, the ZnO/TiO$_2$ interface and the ITO/ZnO interface (including the ZnO resistance). Mane *et al*[22] have prepared nanocrystalline chemical bath deposited TiO$_2$/ZnO thin films on ITO substrates. Owing to low electron effective mass of ZnO (about $0.2m_e$), they have concluded that an increase in ZnO could have a negative effect on the cell performance. They have argued that, because of low electron effective mass, ZnO could affect the electrons injected from the dye, resulting in a poor power conversion efficiency. However, in the present work, the role of TiO$_2$ and ZnO is quite contrary. The electron effective mass of TiO$_2$ is about $1m_e$ that is much higher than ZnO.[23] Hence,

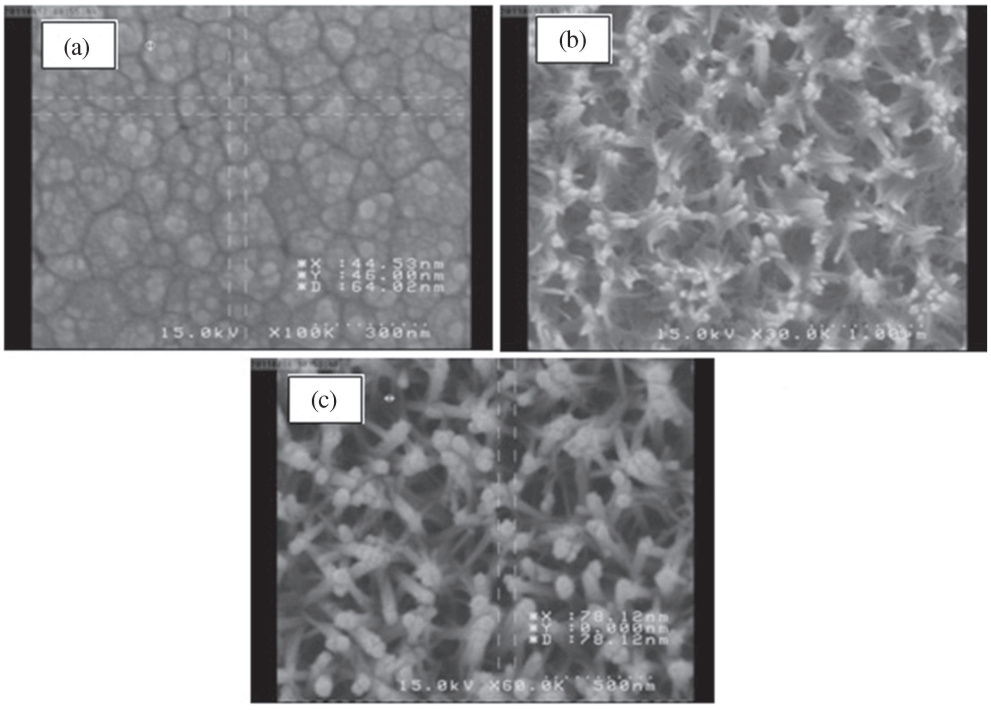

Figure 3. SEM images of (**a**) ZnO seed layer, (**b**) ZnO nanorods and (**c**) ZnO/TiO_2 composite core/shell nanorods.

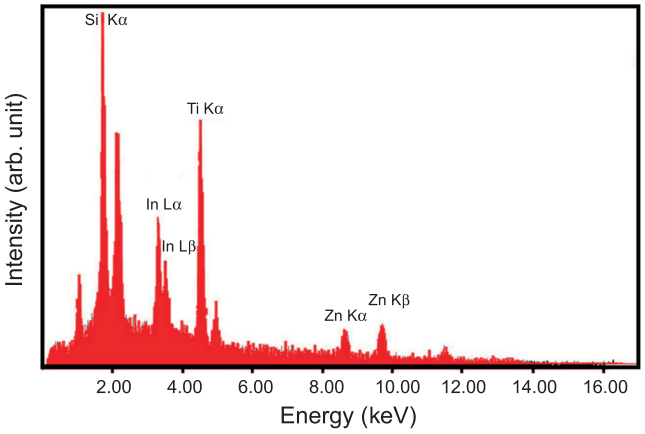

Figure 4. EDX spectrum of ZnO/TiO_2 composite core/shell nanorod thin film (sample number 3) prepared by the sol–gel method.

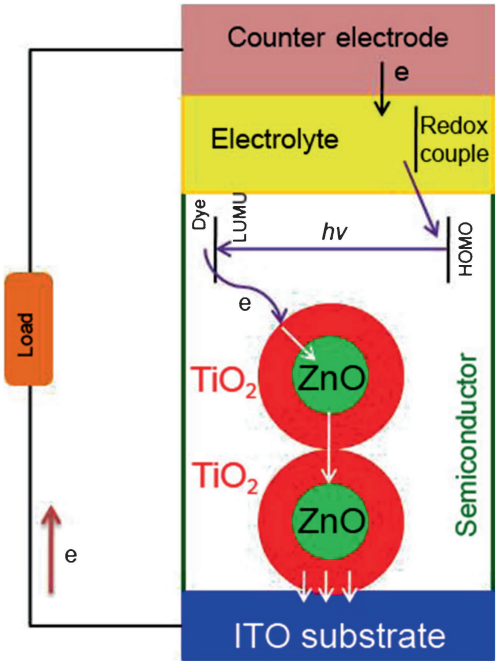

Figure 5. Schematic representation of the electron transport in core/shell model-based dye-sensitized solar cell.

according to the above argument, lower influence of TiO_2 shell on the electrons injected from the dye is expected and consequently better conversion efficiency. To have a measure about the electrical properties of the prepared ZnO/TiO_2 core/shell arrays thin films d.c. electrical resistance (R) and the electrical resistivity (ρ) of the films were measured by the two-probe method. This can be a yardstick for the quality of charge carrier transport in the electrolyte/TiO_2 interface. The measured values are given in table 3. It is seen that the resistance values are in the range of 10^6 Ω which is lower than the values that have been reported in the literature for the sol–gel derived TiO_2 thin films.[24] Meanwhile, we have arranged a comparison between the electrical and optical properties of ZnO/TiO_2 core/shell and bare TiO_2 thin films. To do that, a flat TiO_2 film was deposited on ITO substrate by the sol–gel

Table 3. d.c. electrical resistance and resistivity of the prepared core/shell ZnO/TiO$_2$ thin films.

Sample	R (MΩ)	ρ (Ω cm)
1	9.53	362
2	10	238
3	9.4	316
4	9.99	352
5	9.89	231
6	7.08	177
7	9.79	235
8	10	386
9	10	547
10	9.01	366
11	8.01	237
12	9.57	450
13	6.65	310
14	9.91	491
15	9.64	398
16	9.59	252
17	9.58	182

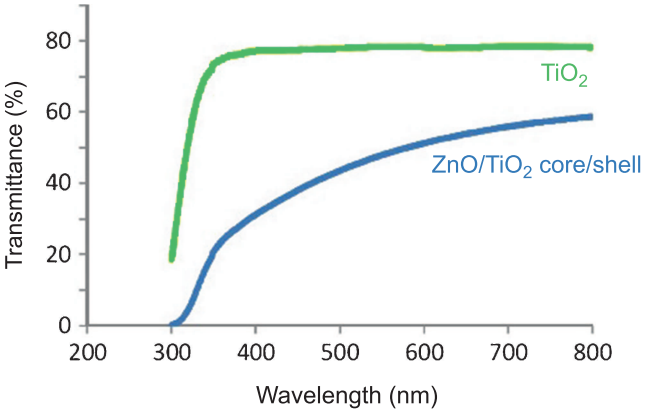

Figure 6. Transmission spectra of TiO$_2$ and ZnO/TiO$_2$ core/shell composite thin films.

dip-coating method. The procedure is as same as in the case of core–shell preparation (sample number 17) except deposition of ZnO core layer. In spite of higher transmission of TiO$_2$ thin film (about 80% in the wavelength range of 400–800 nm, figure 6), it was showed rather high resistivity (∼1194 Ω cm) than ZnO/TiO$_2$ core/shell film. Therefore, it is not suitable as an electron transport layer for being used in inverted solar cells. On the other hand, when pH value of ZnO sol varied from 6.45 to 11.3, the lowest R and ρ obtained in pH = 9.5 and 11.3, respectively. Also, the resistivity decreased with the increase in growing time. Lowest R and ρ were gained in temperatures of 75 and 55°C, respectively. In the meantime, by increasing the annealing temperature from 150 to 450°C both R and ρ decreased. Normally, the crystallinity of the films improves by post-heat treatment that in turn can cause decrease in electrical resistivity owing to narrowing of grain boundaries.[25]

The optical properties of the prepared thin films were also studied. Figure 7a–d shows the transmittance spectra of the prepared films for different pH values, growth times, growth and annealing temperatures in the wavelength range from 200 to 800 nm. The results indicate that the composite thin films are transparent in the visible region of spectrum. Figure 7a-1 illustrates the variation of the film transparency with growth temperature. It can be observed from the figure that when the growth temperature is increased, the film transparency decreases. One possible explanation is that higher growth temperature is beneficial for ZnO to nucleate on the ITO surface, that is to say, it is easier to form plenty of ZnO nuclei at the very beginning of the overgrowth process. Therefore, the adjacent nuclei may fuse together and make larger ones, resulting higher light scattering and equally lower film transparency. In order to determine the absorption band edge of the films, we computed the first derivative of optical transmittance and present this in figure 7a-2. The plots of $dT/d\lambda$ *vs.* wavelength give a peak corresponding to the absorption band edge. As it is obvious, the peak position of the curves shifts to longer wavelengths with growth temperature. This suggests that the absorption band edge shifts from ∼3.74 to ∼3.60 eV with the increase in the growth temperature. On the other hand, the optical transmission of the films increases totally with pH value (figure 7b-1). The increase of the transmission with the increase in pH can be interpreted by a decrease of the film thickness as reported in table 2. An increase of the pH may lead to more OH^- ions in the solution, which incline to combine easily with zinc without leaving enough zinc for ZnO growth on the substrate. This result is also indicated by thickness measurements which show thinner layer at greater pH (table 2). Furthermore, with the increase in pH the absorption band edge of the films shifted toward shorter wavelengths (figure 7b-2). Again, this may be linked to the decrease of film thickness with pH value. With thickness the value of band edge decreases due to energy spread of the localized states increasing.[7] Figure 7c-1 shows the optical transmission spectra of the core/shell ZnO/TiO$_2$ films as a function of the deposition time. It indicates that the films grown at deposition time of 1 h have highest average percentage for transmittance. This sample has the lowest thickness value (240 nm) in comparison to the other ones and having higher transmittance is expected for it. The absorption wavelength values corresponding to the peak positions for the ZnO/TiO$_2$ films did not show remarkable change with growth time (figure 7c-2).

Sol–gel derived thin films that have not been annealed are too impure and too ill-defined to be of use in devices. Figure 7d-1 represents the wavelength dependence of spectral transmittance of the core/shell ZnO/TiO$_2$ thin films deposited by the dip-coating technique and annealed at four different temperatures. All films annealed at different temperatures are transparent in the visible region. As it is clear from the figure, the transparency of the samples increases with the increase of annealing temperature. By increasing the annealing temperature from 150 to 450°C, the film thickness

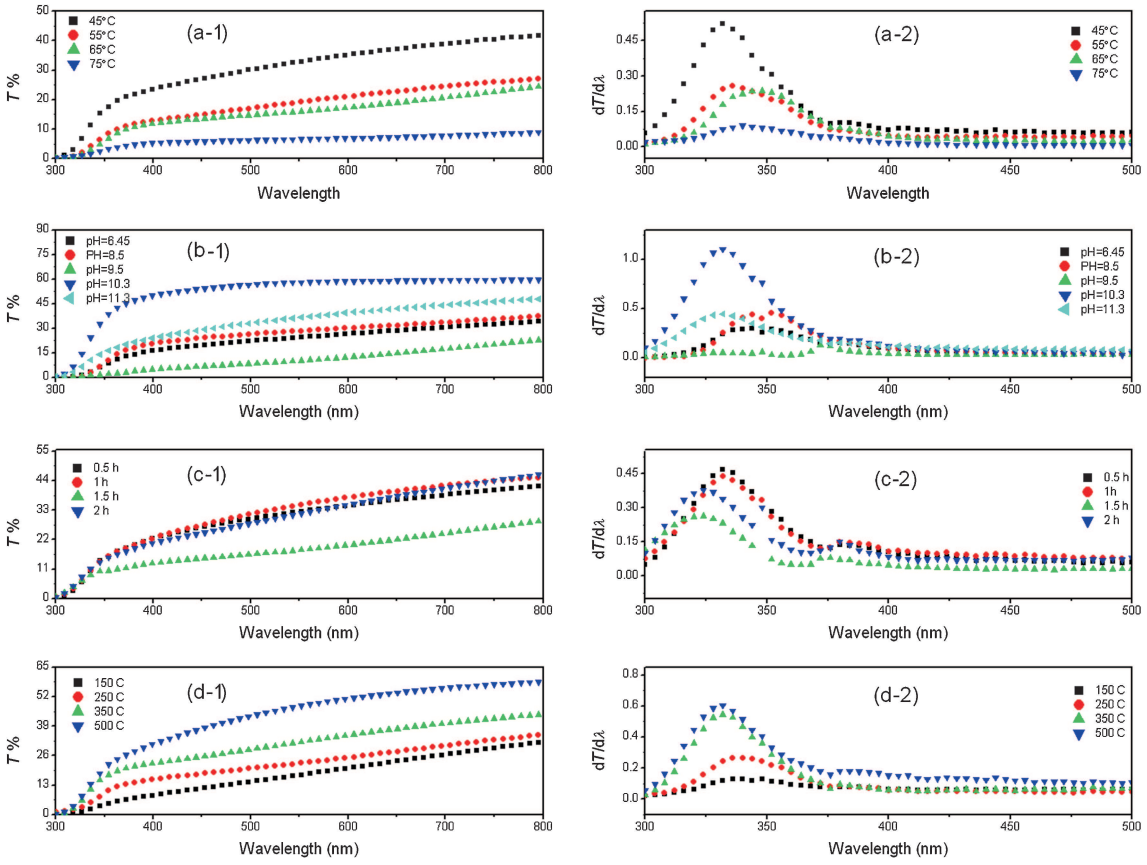

Figure 7. Transmission spectra and pertinent first derivative ($dT/d\lambda$) plots of the prepared samples for different (**a**) pH values, (**b**) growing times, (**c**) growing temperatures and (**d**) annealing temperatures.

decreases from 496 to 190 nm (table 2). Thus the transmittance increases and consequently little light is dispersed in the film.

5. Conclusion

To recapitulate, vertically aligned ZnO nanorod arrays were grown on ITO substrates by the sol–gel dip-coating method and subsequently coated with TiO_2 layer. The XRD result showed the polycrystalline nature of the prepared films with corresponding diffraction peaks for wurtzite hexagonal ZnO and a mixed anatase and rutile structure phase of TiO_2. SEM micrograph of the film confirmed the formation of nanorod arrays on the substrate. EDX analysis revealed the presence of Ti and Zn emission lines along with their corresponding surface values as the constituents of prepared ZnO/TiO_2 core/shell films. By variation of ambient conditions, the optimum values for electrical resistivity and optical transmittance were obtained. The lowest electrical resistivity was obtained about 177 Ω cm at the pH value of 9.5 and the growing temperature of 55°C. Besides, the transmission of the films increased with pH value and annealing temperature. The growing time of 0.5 h had the lowest transmission. Moreover, the bare TiO_2 film was prepared and showed rather high transparency in the visible region of spectrum but the pertinent resistivity was about six times higher than core/shell nanorods.

References

1. Brabec C J and Durrant J R 2008 *MRS Bull.* **33** 670
2. Hsieh C H, Cheng Y J, Li P J, Chen C H, Dubosc M, Liang R M and Hsu C S 2010 *J. Am. Chem. Soc.* **132** 4887
3. Yuekun Lai Y, Gong J and Lin C 2012 *Int. J. Hydrogen Energy* **37** 6438
4. Hau S K, Yip H L and Jen A K Y 2010 *Polym. Rev.* **50** 474
5. Li C Y, Wen T C, Lee T H, Guo T F, Huang J C A, Lin Y C and Hsu Y J 2009 *J. Mater. Chem.* **19** 1643
6. Waldauf C, Morana M, Denk P, Schilinsky P, Coakley K, Choulis S A and Brabec J 2006 *J. Appl. Phys. Lett.* **89** 233517
7. Abdolahzadeh Ziabari A and Ghodsi F E 2011 *Thin Solid Films* **520** 1228
8. Abdolahzadeh Ziabari A and Ghodsi F E 2012 *Surf. Coat. Technol.* **213** 15
9. Abdolahzadeh Ziabari A and Ghodsi F E 2011 *J. Alloys Compd.* **509** 8748
10. Baranyai R, Detrich A, Volentiru E and Horvolgyi Z 2009 *J. Ind. Chem.* **37** 131

11. Abdolahzadeh Ziabari A and Ghodsi F E 2013 *Mater. Sci. Semicond. Process.* **16** 1629
12. Abdolahzadeh Ziabari A and Ghodsi F E 2012 *Sol. Energy Mater. Sol. Cells* **105** 249
13. Abdolahzadeh Ziabari A and Ghodsi F E 2013 *J. Lumin.* **141** 121
14. Cozzoli P D, Kornowski A and Weller H 2003 *J. Am. Chem. Soc.* **125** 14539
15. Zou C W and Gao W 2010 *Trans. Electr. Electron. Mater.* **11** 1
16. Chappel S, Chen S G and Zaban A 2002 *Langmuir* **18** 3336e42
17. Diamant Y, Chen S G, Melamed O and Zaban A 2003 *J. Phys. Chem. B* **107** 1977e81
18. Law M, Greene L E, Radenovic A, Kuykendall T, Liphardt J and Yang P 2006 *J. Phys. Chem. B* **110** 22652
19. Law M, Greene L E, Johnson J C, Saykally R and Yang P D 2005 *Nat. Mater.* **4** 455
20. Baxter J B and Aydil E S 2006 *Sol. Energy Mater. Sol. Cells* **90** 607
21. Baxter J B, Walker A M, Van Ommering K and Aydil E S 2006 *Nanotechnology* **17** S304
22. Mane R S, Lee W J, Pathan H M and Han S H 2005 *J. Phys. Chem. B* **109** 24254
23. Tang H, Prasad K, Sanjinès R, Schmid P E and Lvy F 1994 *J. Appl. Phys.* **75** 2042
24. Haidry A A, Puskelova J, Plecenik T, Durina P, Gregus J, Truchly M, Roch T, Zahoran M, Vargova M, Kus P, Plecenik A and Plesch G 2012 *Appl. Surf. Sci.* **259** 270
25. Abdolahzadeh Ziabari A and Ghodsi F E 2012 *J. Mater. Sci: Mater. Electron.* **23** 1628